European Journal of Chemistry

View Journal Online
View Article Online

Crystal structure and spectral studies of green fluorescent protein (GFP) chromophore analogue ethyl 2-[(4*Z*)-(6-hydroxy naphthalen-2-yl) methylene)-2-methyl-5-oxo-4,5-di hydro-1*H*-imidazol-1-yl] acetate

Anisha Puthuvakkal and Kochunnoonny Manoj *

Photosciences and Photonics, Chemical Sciences and Technology Division, CSIR-National Institute for Interdisciplinary Science and Technology (CSIR-NIIST), Thiruvananthapuram 695019, India
anishap371@gmail.com (A.P.), k.manoj.chem@gmail.com (K.M.)

** Corresponding author at: Photosciences and Photonics, Chemical Sciences and Technology Division, CSIR-National Institute for Interdisciplinary Science and Technology (CSIR-NIIST), Thiruvananthapuram 695019, India.*
Tel: +91.471.2515408 Fax: +91.471.2491712 e-mail: k.manoj.chem@gmail.com (K. Manoj).

RESEARCH ARTICLE

10.5155/eurjchem.10.2.175-179.1869

Received: 10 April 2019
Received in revised form: 19 May 2019
Accepted: 20 May 2019
Published online: 30 June 2019
Printed: 30 June 2019

KEYWORDS

Red shift
Emission
UV absorption
Crystal structure
Fluorescent protein
Intermolecular Interactions

ABSTRACT

Synthetically modified green fluorescent protein chromophore derivative was prepared, its crystal structure and spectral properties were studied. Crystal data for $C_{19}H_{18}N_2O_4$: triclinic, space group *P*-1 (no. 2), *a* = 8.2506(17) Å, *b* = 11.934(2) Å, *c* = 17.461(4) Å, α = 102.89(3)°, β = 94.62(3)°, γ = 96.68(3)°, V = 1654.5(6) Å^3, *Z* = 4, T = 173(2) K, μ(MoKα) = 0.096 mm^{-1}, D_{calc} = 1.358 g/cm^3, 7227 reflections measured (4.722° ≤ 2Θ ≤ 53.996°), 7227 unique (R_{int} = 0.0453, R_{sigma} = 0.0662) which were used in all calculations. The final R1 was 0.0561 (I > 2σ(I)) and wR2 was 0.1658 (all data). The single crystal structure showed, the benzylidine moiety adopts *Z*-conformation in solid state and the molecules were associated by various O–H···O and C–H···O non-covalent interactions. The UV absorption-emission spectral analysis indicated that a significant red shift of emission observed at alkaline pH indicating its utility for live cell imaging applications.

Cite this: *Eur. J. Chem.* **2019**, *10(2)*, 175-179 **Journal website**: www.eurjchem.com

1. Introduction

Discovery of green fluorescent protein (GFP) from jellyfish *Aequorea victoria* provided a powerful tool in the cellular imaging technique due to its wide range of emission colors, photo stability and a low background noise upon UV excitation [1-6]. A number of fluorescence turn-on sensors for various pH, human serum albumin (HSA) and ribonucleic acid (RNA) have been developed using synthetically modified GFP molecules, which exhibit selective high fluorescence, wide range of spectral tunability, high environmental sensitivity and a very low toxicity [7-10]. The high fluorescence quantum yield of the GFP chromophore can be attributed to the non-radiative relaxation of benzylidine imidazolinone (BI) double bond and the exact mechanism of light emission from the GFP proteins have been anticipated to involves a variety of processes such as *E-Z* isomerization, tautomer formation, excited state proton transfer (ESPT), triplet formation, hula-twisting, etc. [11-13]. Although, majority of the literature suggests that GFP chromophore and its analogues exhibit high fluorescence due to the tautomerization as well as restricted *Z*-conformation (Scheme 1) of benzylidene imidazolinone (BI) moiety and it undergo excited state *E-Z* twisting in solutions that triggers internal conversion making them weakly emissive [14,15].

The concept of inhibiting the free rotation of the aryl-alkene bond of GFP chromophore for efficient fluorescence, various synthetic strategies has been explored. Baldridge *et al*. investigated a reversible locking of BI moiety by pyridyl substitution, which produces selective 'turn on' fluorescence in the presence of Zn^{2+} or Cd^{2+} ions [16]. Wu and Burgess developed another approach by using a Lewis acid (BF_2 group), which connect the benzylidine and imidazolinone ring to restrain the twisting, resulted a strong fluorescence in solutions [17]. Chen *et al*. synthesized various *ortho*-hydroxylated GFP derivatives, which gave high emission in the solid state through intramolecular excited-state proton transfer (ESPT) pathways [18]. Tolbert *et al*. reported hydrophobic derivatives of the GFP chromophore that exhibits fluorescence in the solid due to the aggregation induced emission [19].

http://dx.doi.org/10.5155/eurjchem.10.2.175-179.1869

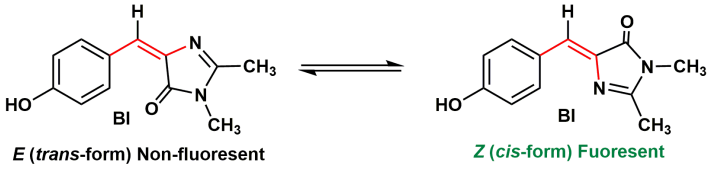

Scheme 1

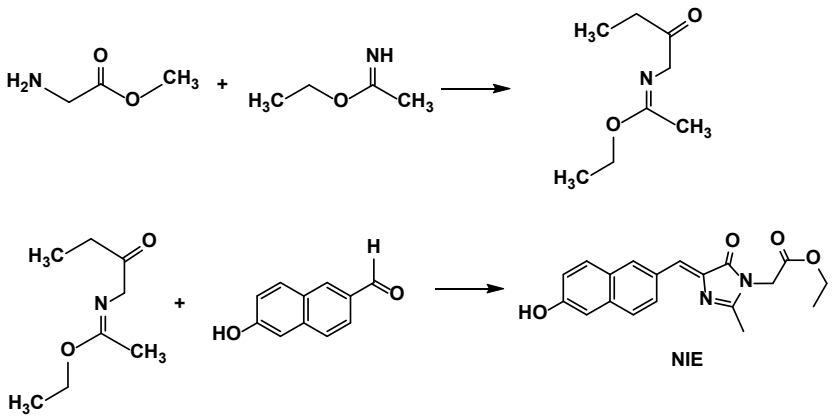

Scheme 2

Chou *et al*. come up with a double locking of GFP chromophore to its *Z*-form by five-membered ring cyclization, from which the excited-state intramolecular proton transfer takes place, produced a very high quantum yield and has been successfully applied to fabricate a yellow organic light emitting diodes (OLED) [20]. In order to achieve the emissive form of BI, we used a new design strategy that involved aromatic ring expansion leading to the preparation of ethyl 2-[(4*Z*)-(6-hydroxy naphthalen-2-yl) methylene)-2-methyl-5-oxo-4,5-di hydro-1*H*-imidazol-1-yl] acetate (**NIE**).

2. Experimental

All chemicals and reagents were purchased from commercial sources and used without further purification. NMR spectra were measured on a 500 MHz Bruker Avance DPX NMR instrument and IR spectra recorded on a Shimadzu IR Prestige-21 spectrophotometer with sample on KBr. High resolution mass spectra (HR-MS) were measured on a Bruker microTOF II instrument using electron spray ionization (ESI). UV-VIS spectra were recorded with a Varian Cary 100 spectrophotometer. The fluorescence spectra were performed on a Hitachi F-4500 fluorescence spectrophotometer.

2.1. Synthesis

Methyl glycinate hydrochloride (5 mmol, 625 mg) and K_2CO_3 (5 mmol, 691 mg) were suspended in di ethyl ether (125 mL), followed by addition of water (20 mL) then addition of ethyl acetimidate hydrochloride (5 mmol, 698 mg). The mixture was shaken for 6 min then the ether was decant off. An additional portion of di ethyl ether (75 mL) was added, the mixture was shaken for 6 min then the di ethyl ether was decant off. The combined organic portions were dried over anhydrous $MgSO_4$ and the solvent was removed *in vacuo* to give imidate, which further mix with the Schiff base of 6-hydroxy 2-napthaldehyde (5 mmol, 860 mg) at room temperature for 12 h (Scheme 2). The residue obtained was finally purified by flash column chromatography on a silica gel (230-400 mesh) using ethyl acetate-hexane (1:2) mixture.

Ethyl 2-[(4Z)-((6-hydroxy naphthalen-2-yl) methylene)-2-methyl-5-oxo-4,5-di hydro-1H-imidazol-1-yl] acetate (**NIE**): Yield: 912 mg, 54%. M.p.: 206-207 °C. FT-IR (KBr, ν, cm^{-1}): 1697, 1741 (C=O), 3319 (OH). ^{1}H NMR (500 MHz, $CDCl_3$, δ, ppm): 1.31 (t, 3H, *J* = 7.9 Hz, CH_3), 2.38 (s, 3H, Im-CH_3), 4.23-4.28 (q, 2H, *J* = 4.2 Hz, CH_2), 4.41 (s, 2H, CH_2), 5.41 (s, 1H, Ar-OH), 7.10-7.11 (d, 1H, *J* = 11.4 Hz, Ar-H), 7.13 (d, 1H, *J* = 2.2 Hz, Ar-H), 7.27 (s, 1H, CH), 7.68 (d, 1H, *J* = 9.1 Hz, Ar-H), 7.81 (d, 1H, *J* = 8.8 Hz, Ar-H), 8.38 (t, 2H, *J* = 9.5 Hz, Ar-H). ^{13}C NMR (125 MHz, $CDCl_3$, δ, ppm): 14.13, 15.59, 41.45, 55.96, 56.31, 56.47, 61.99, 96.02, 109.72, 114.93, 115.20, 122.43, 135.42, 143.30, 152.63, 155.60, 158.99, 167.78, 170.07. HRMS (EI, *m*/*z*) calcd. for $C_{19}H_{18}N_2O_4$: 338.13; found: 339.13 [NIE+H$^+$].

2.2. Crystallographic details

X-ray intensity data were collected on a Bruker SMART APEX II CCD Diffractometer in omega and phi scan mode, $\lambda_{MoK\alpha}$ = 0.71073 Å at low temperature (173 K) using OXFORD LN2 cryosystem. All the intensities were corrected for Lorentz-polarisation and absorption effects using Bruker's SAINT and SADABS programs [21]. The crystal structures were solved by Direct methods using program SHELXT-2014 [22]; the full-matrix least squares refinements on F^2 were carried out by using SHELXL-2014 [23]. Hydrogen atoms were included in the refinement as per the riding model. Table 1 summarizes the crystallographic data for **NIE**.

3. Results and discussion

3.1. Crystal structure

Yellow crystals of **NIE** were obtained by dissolving the compounds in dichloromethane:methanol (3:1, *v*:*v*) mixture and slow evaporation at room temperature. Suitable needle crystals of **NIE** were selected for the single X-ray diffraction studies. The single crystal XRD analysis indicated that the **NIE** crystals belong to triclinic, *P*–1 and the asymmetric unit containing two molecules that are labeled with *A* & *B* numbering scheme (Figure 1).

Table 1. Summary of crystallographic data.

Parameters	**NIE**
CCDC No.	1902393
Empirical formula	$C_{19}H_{18}N_2O_4$
Formula weight	338.35
Temperature (K)	173
Crystal system	Triclinic
Space group	*P*–1
a (Å)	8.2506(17)
b (Å)	11.934(2)
c (Å)	17.461(4)
α (°)	102.89(3)
β (°)	94.62(3)
γ (°)	96.68(3)
Volume (Å^3)	1654.5(6)
Z	4
ρ_{calc} (g/cm^3)	1.358
μ (mm^{-1})	0.96
F(000)	712.0
Crystal size (mm^3)	0.25 × 0.10 × 0.05
Radiation	MoKα (λ = 0.71073)
2Θ range for data collection (°)	4.722 to 53.996
Index ranges	$-10 \le h \le 10$, $-15 \le k \le 14$, $-22 \le l \le 22$
Reflections collected	7227
Independent reflections	5031 [R_{int} = 0.066]
Data/restraints/parameters	7227/0/456
Goodness-of-fit on F^2	0.995
Final R indexes [I≥2σ (I)]	R_1 = 0.0561, wR_2 = 0.1390
Final R indexes [all data]	R_1 = 0.0947, wR_2 = 0.1658
Largest diff. peak/hole (e.Å^{-3})	0.28/-0.32

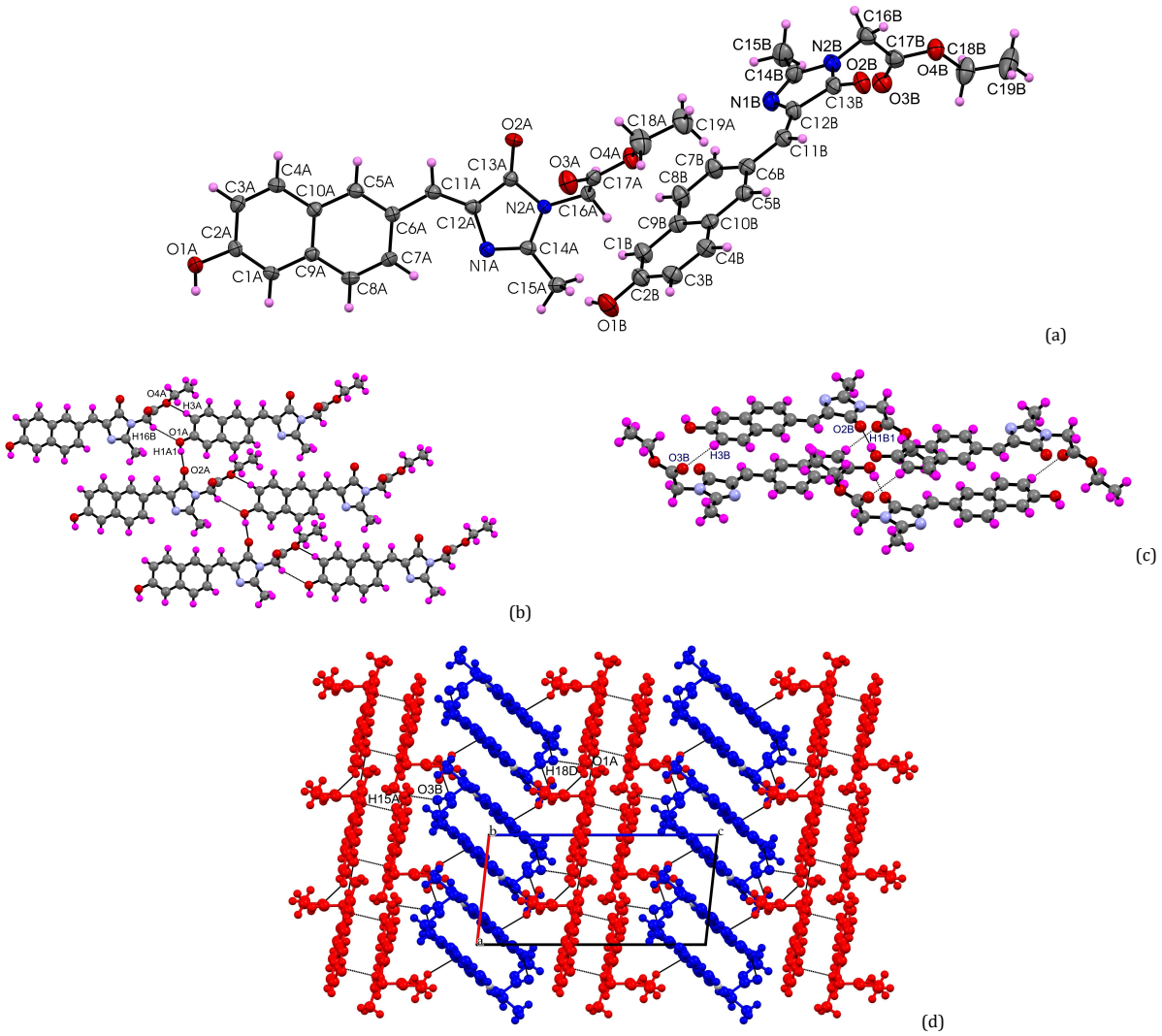

Figure 1. (**a**)Molecular structure of the compound showing the atom-numbering scheme, (b) Molecular layers of molecule A, (c) Molecular layers of molecule B and (d) crystal packing of **NIE** crystal.

Table 2. Geometrical parametersof hydrogen bonding interaction in crystals of **NIE**.

D–H···A	H···A (Å)	D···A (Å)	D–H···A (°)	Symmetry code
C3*A*–H3*A*···O4*A*	2.62	3.438(4)	147	*x*+1, *y*-1, *z*
C3*B*–H3*B*···O3*B*	2.53	3.331(4)	145	-*x*, -*y*-1, -*z*
C15*A*–H15*A*···O3*B*	2.52	3.366(4)	148	*x*-1, *y*+1, *z*
C15*B*–H15*D*···O3*B*	2.60	3.244(5)	125	*x*, *y*, *z*
C16*B*–H16*D*···O3*A*	2.51	3.151(4)	123	*x*+1, *y*-1, *z*
C18*B*–H18*D*···O1*A*	2.56	3.389(5)	144	*x*, *y*, *z*
O1*A*–H1*A*1···O2*A*	1.92	2.718(3)	166	*x*, *y*-1, *z*
O1*B*–H1*B*1···O2*B*	1.97	2.785(4)	178	*x*, *y*-1, *z*

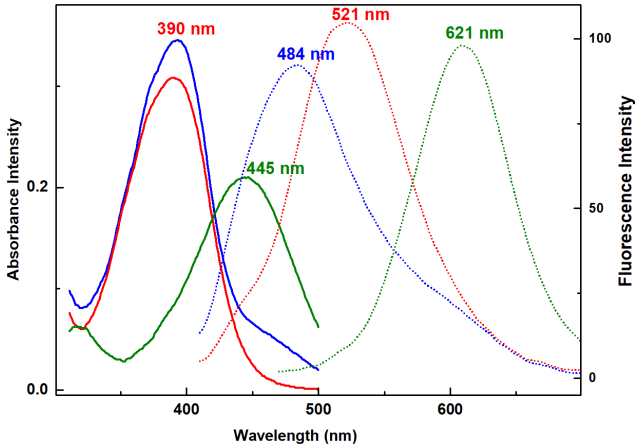

Figure 2. Absorption (line) and emission spectra (dotted line) of **NIE** in solution. Color codes: Blue = MeOH, Red = Methanol acidified with trifluoro acetic acid and Green = Methanol solution with butyl amine.

The benzylidine and imidazole moiety of both molecules was in the same plane according to *Z*-conformation (Figure 1a), which is the fluorescent emissive form of Green Fluorescent Protein (GFP) chromophore as discussed earlier. The molecules of *A* were translated to form a chain like arrangement *via* C3*A*–H3*A*···O4*A* and C16*A*–H16*B*···O1*A* interactions [24-26] diagonal to *ab*-plane (Figure 1b). Such two chains extended to form a double layer (red in Figure 1d) along the *c*-axis using the hydrogen bonds O1*A*–H1*A1*···O2*A* (Table 2). Similarly, the other asymmetric molecules of *B* associated to form a chain like arrangement using O1*B*–H1*B1*···O2*B* hydrogen bonds along the *b*-axis (Figure 1c). Two such chains further extended to form double layer (blue color in Figure 1d) *via* weak non-covalent interactions C3*B*–H3*B*···O3*B* and C16*B*–H16*D*···O2*A* diagonal to *ac*-plane (Table 2). These molecular layers together to form a ladder like close packing, *via* C15*A*–H15*A*···O3*B* and C16*B*–H16*D*···O3*A* (Figure 1d and Table 2).

3.2. Spectral studies

The absorption emission spectral variation observed with the **NIE** and the effect of pH studied (Figure 2). In methanol solution, **NIE** has absorption maximum of 390 nm and fluorescence emission maximum at 484nm resulting green emission. Upon acidification with trifluoro acetic acid (pH = 2.5), the protonated **NIE** species have similar absorption maximum (390 nm), whereas the emission maximum shifted to 521 nm with yellowish green color. However, in alkaline condition (pH= 10.8, using butyl amine addition), absorption maximum changed to 445 nm due to the deprotonation of **NIE** hydroxyl group and its respective emission shifted to orange fluorescence (621 nm). It is interesting to note that depending on the pH, the fluorescence emission of **NIE** changed from green to orange can be used for the pH sensor application of live cell imaging.

4. Conclusion

We have synthesized a new GFP analogue, **NIE** and carried out its spectral characterization and crystal structure. The single crystal structure analysis of **NIE** indicated that the molecule adopts *Z*-conformation in its crystal lattice, which is the fluorescent emissive form of the GFP chromophore that are associated by non-covalent interactions of O–H···O and C–H···O. The fluorescence emission of **NIE** was found to be significantly red shifted under alkaline conditions, which can be used as pH sensor applications for live cell imaging and studies are exploring further in this direction.

Acknowledgements

We thank Kerala State Council for Science, Technology and Environment (KSCSTE), Thiruvananthapuram, India for the financial support under the Varghese Kurien Young Scientist Scheme (Ref. No. 004/YSS/CS/KM/2013/KSCSTE). We gratefully acknowledge Dr. A. Ajayagosh, Director, CSIR-NIIST for his encouragement and support. We acknowledge Prof. K. M. Sureshan and Mr. Alex for the Single Crystal XRD data collection at IISER-Thiruvananthapuram.

Supporting information

CCDC-1902393 contains the supplementary crystallographic data for this paper. These data can be obtained free of charge via https://www.ccdc.cam.ac.uk/structures/, or by e-mailing data_request@ccdc.cam.ac.uk, or by contacting The Cambridge Crystallographic Data Centre, 12 Union Road, Cambridge CB2 1EZ, UK; fax: +44(0)1223-336033.

Disclosure statement

Conflict of interests: The authors declare that they have no conflict of interest.
Author contributions: All authors contributed equally to this work.

Ethical approval: All ethical guidelines have been adhered.
Sample availability: Samples of the compounds are available from the author.

Funding

Kerala State Council for Science, Technology and Environment
http://dx.doi.org/10.13039/501100006144

ORCID

Anisha Puthuvakkal
http://orcid.org/0000-0001-6385-3113
Kochunnoonny Manoj
http://orcid.org/0000-0002-1511-1091

References

[1]. Shimomura, *FEBS Lett.* **1979**, *104*, 220-222.
[2]. Zimmer, M. *Chem. Rev.* **2002**, *102*, 759-782.
[3]. Giepmans, B. N. G.; Adams, S. R.; Ellisman, M. H.; Tsien, R. Y. *Science* **2006**, *312*, 217-224.
[4]. Chalfie, M. *Angew. Chem. Int. Ed.* **2009**, *48*, 5603-5611.
[5]. Chudakov, D. M.; Matz, M. V.; Lukyanov, S.; Lukyanov, K. A. *Physiol. Rev.* **2010**, *90*, 1103-1163.
[6]. Chang, J.; Chen, X.; Glass, Z.; Gao, F.; Mao, L.; Wang, M.; Xu, Q. *Acc. Chem. Res.* **2019**, *52*, 665-675.
[7]. Kneen, M.; Farinas, J.; Li, Y.; Verkman, A. S. *Biophys. J.* **1998**, *74*, 1591-1599.
[8]. Tamura, T.; Hamachi, I. *ACS Chem. Biol.* **2014**, *9*, 2708-2717.
[9]. Walker, C. L.; Konstantin A Lukyanov, K. A.; Yampolsky, I. V.; Mishin, A. S.; Bommarius, A. S.; Duraj-Thatte, A. M.; Azizi, B.; Tolbert, L. M.; Solntsev, K. M. *Curr. Opin. Chem. Biol.* **2015**, *27*, 64-74.
[10]. Wang, Z.; Luo, Y.; Xie, X.; Hu, X.; Song, H.; Zhao, Y.; Shi, J.; Wang, L.; Glinsky, G.; Chen, N.; Lal, R.; Fan, C. *Angew. Chem. Int. Ed.* **2018**, *57*, 972-976.
[11]. Meech, S. R. *Chem. Soc. Rev.* **2009**, *39*, 2922-2934.
[12]. Tolbert, L. M.; Baldridge, A.; Kowalik, J.; Solntsev, K. M. *Acc. Chem. Res.* **2010**, *45*, 171-181.
[13]. Chatterjee, T.; Lacombat, F.; Yadav, D.; Mandal, M.; Plaza, P.; Espagne, A.; Mandal, P. K. *J. Phys. Chem. B.* **2016**, *120,* 9716-9722.
[14]. Dong, J.; Abulwerdi, F.; Baldridge, A.; Kowalik, J.; Solntsev, K. M.; Tolbert, L. M. *J. Am. Chem. Soc.* **2008**, *130,* 14096-14098.
[15]. Wang, D.; Merz, T.; Van Gunsteren, W. F. *Phys. Chem. Chem. Phys.* **2010**, *12,* 11051-11061.
[16]. Baldridge, A.; Solntsev, K. M.; Song, C.; Tanioka, T.; Kowalik, J.; Hardcastle, K.; Tolbert, L. M. *Chem. Commun*. **2010**, *46*, 5686-5688.
[17]. Wu, L.; Burgess, K. *J. Am. Chem. Soc*. **2008**, *130*, 4089-4096.
[18]. Chen, K.; Cheng, Y.; Lai, C.; Hsu, C.; Ho, M.; Lee, G.; Chou, P. *J. Am. Chem. Soc*. **2007**, *129*, 4534-4535.
[19]. Dong, J.; Solntsev, K. M.; Tolbert, L. M. *J. Am. Chem. Soc.* **2009**, *131,* 662-670.
[20]. Hsu, Y.; Chen, Y.; Tseng, H.; Zhang, Z.; Shen, J.; Chuang, W.; Lin, T.; Lee, C.; Hung, W.; Hong, B.; Liu, S.; Chou, P. *J. Am. Chem. Soc*. **2014**, *136*, 11805-11812.
[21]. Bruker. *APEX2*, *SAINT* and *SADABS*. Bruker AXS Inc., Madison, Wisconsin, USA, 2011.
[22]. Sheldrick, G. M. *Acta Cryst. A* **2015**, *71*, 3-8.
[23]. Sheldrick, G. M. *Acta Cryst. C* **2015**, *71*, 3-8.
[24]. Manoj, K.; Gonnade, R. G.; Bhadbhade, M. M.; Shashidhar, M. S. *Cryst. Growth Des*. **2006**, *6*, 1485-1492.
[25]. Manoj, K.; Gonnade, R. G.; Bhadbhade, M. M.; Shashidhar, M. S. *Acta Crystallogr. C* **2009**, *65*, o335-o338.
[26]. Manoj, K.; Gonnade, R. G.; Bhadbhade, M. M.; Shashidhar, M. S. *CrystEngComm* **2012**, *14*, 1716-1722.